Electrochemical Properties of Electroactive Monolayers Having $[Os(bpy)_3]^{2+}$ Moieties

Gyeong Sook Bang and Il Cheol Jeon*

Department of Chemistry, Jeonbuk National University, Jeonbuk 561-756, Korea
Received May 27, 2000

Self-assembled monolayers (SAMs) of the alkylthiols with $[Os(bpy)_3]^{2+}$ moiety at the terminal position were prepared on gold electrode surface. Examination of the cyclic voltammograms for the SAM shows that it does not organize well unlike alkylthiols, which is attributed to the much larger diameter of $[Os(bpy)_3]^{2+}$ moiety compared with the cross-section of alkyl chains and the distance between the adsorption sites. Electromicrogravimetry study shows that the hydration numbers of the electrolyte were 16 ± 2, 11 ± 1, 5 ± 1 and 24 ± 6 for ClO_4^-, PF_6^-, NO_3^-, and SO_4^{2-}, respectively. The binary SAMs of alkylthiols with $[Os(bpy)_3]^{2+}$ terminal-group were prepared by co-adsorption of alkylthiols as spacer molecules, which results in better packing in SAM and accordingly the stability was enhanced.

Keywords : SAM, $[Os(bpy)_3]^{2+}$, Alkanethiol, EQCM, Hydration number.

Introduction

The SAMs on electrode surfaces are of important interest as a model system for studies of interfacial electron transfer.[1-4] The terminal functional groups on SAMs are attractive for applications of sensor[5] and oriented films as well as for the modification of surface properties such as nanotribology,[6] wetting,[7,8] and adhesion.[5,9-21] Utilization of self-assembled monolayers having terminal functional groups is usually based on the information about packing, stability, electron transfer and so forth, which the SAMs of simple *n*-alkylthiols exhibit. Generally, the functional groups at the end position are larger than methyl group of simple alkylthiols. The SAMs having large tail groups would not pack with good ordering as alkylthiols because of much-reduced repulsion between backbones of the nearest adsorbents[22] which is attributed to larger separation compared with that of alkylthiol SAMs. Thus, the enhancement of the packing or ordering of the SAM having large tail group is required. Co-adsorption of small adsorbents such as n-alkylthiols with proper chain length is expected to be advantageous for dense packing.

In fact, there are some previous reports from which enhancement of self-assembly in packing is seemed to be achieved by co-adsorption.[23,24] As a continuing endeavor for the study of SAMs with large terminal groups, we presented recently about the packing of the binary SAMs of fullerene-terminated alkylthiols and *n*-alkylthiols studied by scanning tunneling microscopy.[25,26] It would be interesting to understand the effect of the tail group charge on the packing and orderings of the SAMs. For a comparison with the neutral tail group cases, we prepared a monolayer composed of $[Os(bpy)_2L]^{2+}$, where L denotes the 4-methyl-4'-alkanethiol-bipyridyl ligand, shortly bpy-CnSH, and the subscript n denotes the number of carbon atoms in the alkyl chain. Alkylthiols were also used as spacers in making the binary SAMs having bulky $[Os(bpy)_3]^{2+}$ moieties and the effect of the spacer was studied.

As a trial for understanding of the electrochemical properties of the monolayer, we performed electrochemical microgravimetry to investigate the current response accompanying the redox process of a $[Os(bpy)_2(bpy\text{-}CnSH)]^{2+}$ on gold and the corresponding mass transport due to the movement of counter-anions toward and away from the SAM. The measured electrochemical response comes from the redox reaction of the adsorbed species, assuming that variation in the double layer charging current is small. In this regard, several groups have interests on the electrostatic interaction between the terminal functional group on the electrode surface and the anions in solution.[6,14,27-32]

In this article the electrogravimetric behaviors of the SAM electrodes are reported. In addition, the effect of spacer molecules on the voltammetric response of the mixed SAMs is described and the hydration numbers of the electrolyte anions at the $[Os(bpy)_2(bpy\text{-}CnSH)]^{2+}$ modified gold electrode in several supporting electrolyte solutions are accounted for.

Experimental Section

Materials. All the commercial chemicals and solvents were used as received. De-ionized water (resistivity > 18 MΩ cm) was used throughout the experiment. $HClO_4$, $NaClO_4$, H_2SO_4, KPF_6, and KNO_3 were used as the supporting electrolytes.

4-Methyl-4'-alkanethiol-bipyridyls (bpy-C_{13}SH and bpy-C_5SH) were synthesized according to the Scheme 1, which is described in detail by Moon.[33] To prepare 4-methyl-4'-tridecanethiol-bipyridyl (Aldrich), LDA was reacted with 4,4-dimethyl-2,2'-bipyridyl and the reaction with 1,4-dibromobutane (Aldrich) was followed to yield 4-methyl-4'-bromopentyl-2,2'-bipyridyl. Then bromide was converted to thio-

*Corresponding author: Fax: +82-63-270-3408, e-mail: icjeon@moak.chonbuk.ac.kr

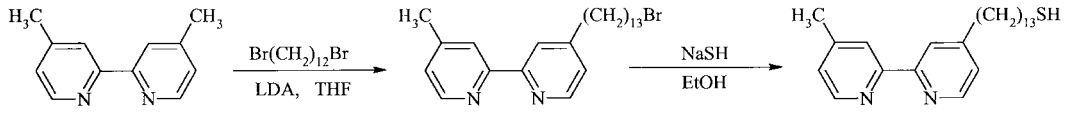

Scheme 1. Synthesis of 4-methyl-4'-tridecanethiol-bipyridyl (bpy-$C_{13}SH$).

acetate, then thiol by hydrolysis. The product was characterized with mass spectrometry and nuclear magnetic resonance spectroscopy. Yield: 22%.

To yield $[Os(bpy)_2(bpy\text{-}C_{13}SH)](PF_6)_2$. $[Os(bpy)_2Cl_2]$ was treated with 4-methyl-4'-tridecanethiol-bipyridyl in ethylene glycol at 240 °C under nitrogen atmosphere for 6 h. After heating at reflux, the solution is allowed to cool to room temperature for 1 h. An equal volume of saturated aqueous NH_4PF_6 was added to induce precipitation. The solid was collected by suction and washed with water and dried in vacuo at 60-70 °C. Yield: 86%. $[Os(bpy)_2(bpy\text{-}C_{13}SH)]^{2+}$ was characterized successfully by mass spectrometry and nuclear magnetic resonance spectroscopy.[34,35]

The monolayers were formed on the electrode by soaking the electrode in a methanol solution containing 2 mM $[Os(bpy)_2(bpy\text{-}C_{13}SH)]^{2+}$ for 24 h, followed by rinsing thoroughly with methanol and drying with a stream of nitrogen gas, and then used in electrochemical measurements.

Apparatus. Cyclic voltammograms were obtained using a commercial potentiostat (BAS 100B/W). Electrochemical microgravimetry was performed by using a lab-made electrochemical quartz crystal microbalance (EQCM) with a Kel-F based cell.[36] Quartz Crystal Microbalance (QCM) was used to monitor the adsorption kinetics at ambient condition with no potential applied to the quartz crystal of EQCM.

A Ag(s)|AgCl(s)|KCl(sat.) reference electrode and a Pt wire was used as a counter electrode. AT-cut quartz crystals (10.0 MHz) were purchased from International Crystal Manufacturer Inc., Oklahoma, OK. The total area exposed to the solution of gold electrode was *ca.* 0.2 cm^2.

Results and Discussion

Adsorption kinetics. With the aid of a quartz crystal microbalance (QCM), adsorption of the complexes was observed by monitoring the frequency decrease, which is equivalent to the increase in mass on the electrode surface. Figure 1 shows that the gold surface of a quartz crystal oscillator immersed in a 10^{-4} M $[Os(bpy)_2(bpy\text{-}C_{13}SH)]^{2+}$ solution was covered to almost a full coverage in 10 min. The adsorption kinetics of $[Os(bpy)_2(bpy\text{-}C_{13}SH)]^{2+}$ in methanol can be fit with the adsorption model,[2,37] which leads to

$$\theta = C\{1 - \exp[(-k_a/N_o)(C + K)t)]\}/(C + K),$$

where θ is the fractional surface coverage and C is the bulk concentration of $[Os(bpy)_2(bpy\text{-}C_{13}SH)]^{2+}$ in molarity. The adsorption equilibrium constant $K = k_d/k_a$, where k_d and k_a are the desorption and adsorption rate constants, respectively. N_o is the surface adsorbent concentration at full coverage, and t is the adsorption time. The solid line shows a

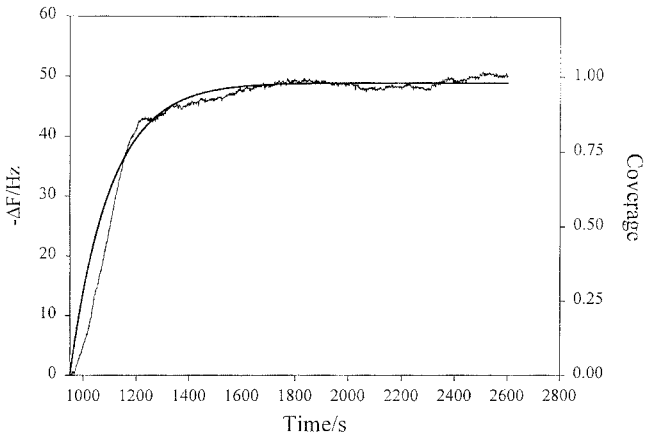

Figure 1. Adsorption data for 0.1 mM $[Os(bpy)_2(bpy\text{-}C_{13}SH)](PF_6)_2$ in methanol and the fitting curve using a set of appropriate kinetic parameters, that is, $k_a = 65\ M^{-1}\ s^{-1}$, $k_d = 1.3 \times 10^{-4}\ s^{-1}$, $K = 2 \times 10^{-6}$, and $\Delta G^\circ = -7.8$ kcal mol^{-1}.

fitting curve according to the equation yielding k_a, k_d, and K value of 65 M^{-1} sec^{-1}, 1.3×10^{-4} sec^{-1}, and 2×10^{-6} M, respectively. From these values, the energy of adsorption is determined for $[Os(bpy)_2(bpy\text{-}C_{13}SH)]^{2+}$ monolayers on gold as -7.8 kcal mol^{-1}.

The electrochemical response of $[Os(bpy)_2(bpy\text{-}C_{13}SH)]^{2+}$ SAM. At first, the electrochemical response was examined by measuring cyclic voltammograms of the $[Os(bpy)_2(bpy\text{-}C_{13}SH)]^{2+}$ SAM. Figure 2 shows the cyclic voltammograms of the SAM in several electrolytes and the summarized electrochemical data are shown in Table 1. The peak current increased quite linearly with the scan rate, which is the characteristic of the immobilized species.

The formal potential in 0.05 M H_2SO_4 is 0.79 V while those measured in KPF_6 and $HClO_4$ are 0.69 V. The formal potential of the model compound $[Os(bpy)_3]^{2+}$ is 0.67 V. During the oxidation process, the Gibbs energy difference in H_2SO_4 with respect to the model compound is calculated to be about -3.0 kcal mol^{-1} while that in $HClO_4$ is smaller than 0.5 kcal mol^{-1}. Hence, the SAM in 0.05 M H_2SO_4 is believed to be more strongly adsorbed than that in other electrolytes.

Regarding the peak separation, it is about 40 mV in 0.1 M $HClO_4$ while it is about 55 mV in 0.05 M H_2SO_4. Thus the electrode covered with the SAM in H_2SO_4 is thought to be more resistive than those in other electrolyte solutions. When the scan rate is lower than 2 V s^{-1}, the peak separation is almost constant and it increases along with the scan rate when they are higher than this value. Generally it is known that there are no kinetic limitations for redox processes of a surface-immobilized species if the peak separation is smaller than 30 mV and constant with the scan rate.[1] Thus, the elec-

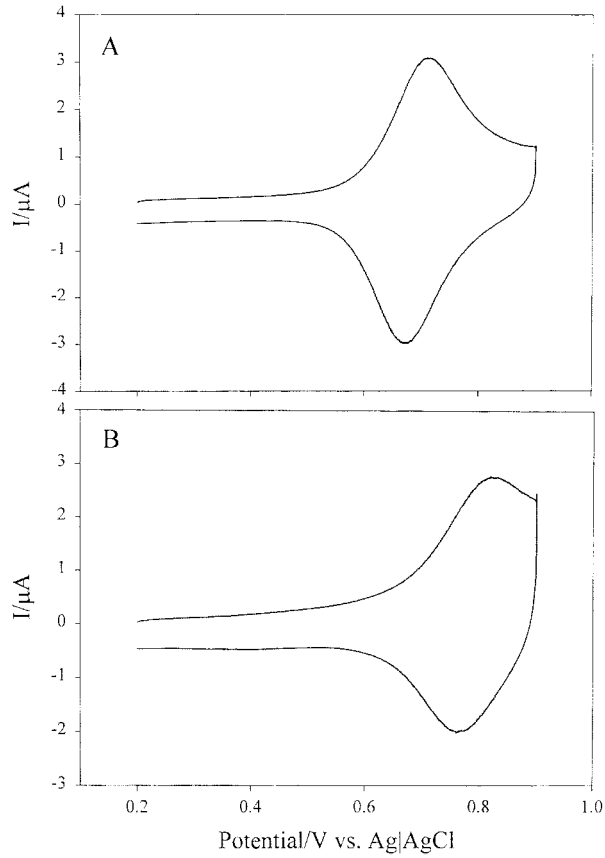

Figure 2. Cyclic voltammograms of a $[Os(bpy)_2(bpy\text{-}C_{13}SH)]^{2+}$ SAM in (A) 0.1 M $HClO_4$, and (B) 0.05 M H_2SO_4 recorded at 0.1 V s^{-1}.

tron transfer is seemed to be somewhat limited in the SAM electrode, however, the electron transfer rate does not decrease if the scan rate is higher than 2 V s^{-1}.

In 0.1 M $HClO_4$ the ΔE_{fwhm} values are about 155 and 125 mV, respectively for the oxidation and the reduction processes. These values are larger than the theoretical value of 90.6/n mV implying repulsion interaction between neighbors, where *n* is the mole number of electrons transferred. When ΔE_{fwhm} values are larger than 90.6/n mV, it is indicative of the repulsion between electroactive centers or higher degree of organization in the monolayer, whereas smaller values indicate attractive or stabilizing interactions.[5,38-41] Thus, it is understood that there are repulsive interactions in the SAM. The fact that the anodic wave is broader than the cathodic one can be understood intuitively as a higher degree of repulsion between the trivalent oxidized species than that between the divalent reduced species.[5] In 0.05 M H_2SO_4 case, ΔE_{fwhm} is estimated to be much broader, however, it is not possible to measure exactly in sulfuric acid medium because the peaks are too broad. Anyhow, it can be explained as sulfate ions among the examined electrolytes induce the largest changes in structure, solvation, and environment of the monolayer when they are associated with the SAM.

Stability of the SAM upon potential cycling. The anodic or cathodic peak currents measured in different electrolyte solutions were integrated to calculate the coverage. Integration of the oxidation current yields the coverage to be 1.3 $(\pm 0.2) \times 10^{-10}$ mol cm^{-2}. If the roughness factor of the gold surface were 1.2,[42] the coverage is 1.0×10^{-10} mol cm^{-2}. This value corresponds to 100% of a full monolayer (1.0×10^{-10} mol cm^{-2}) by assuming the hexagonal close packing and a diameter of $[Os(bpy)_3]^{2-}$ to be 12 Å.[43,44] The estimated coverage from the cathodic wave is larger than that from the anodic wave. The more positive the anodic peak potential is, the more the coverage values deviate. In the 0.05 M H_2SO_4 solution case, the coverage estimated from the anodic wave is just 20% of that from the cathodic wave. It is due to the difficulty in assessing the baseline because of the high and curved background current in the positive potential region.

The stability of the SAM was tested by cycling the poten-

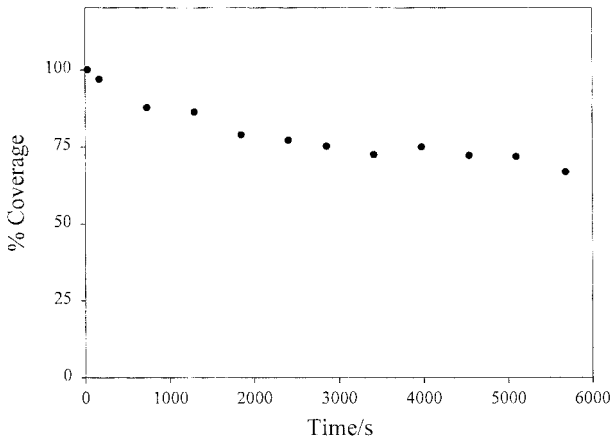

Figure 3. Variation of surface coverage of a $[Os(bpy)_2(bpy\text{-}C_{13}SH)]^{2-}$ SAM electrode measured in 0.1 M $NaClO_4$ during repetitive potential cycling at 0.1 V s^{-1}. After 1.5 h the coverage was decreased to 75% of the initial value.

Table 1. Electrochemical data for the $[Os(bpy)_2(bpy\text{-}C_{13}SH)]^{2-}$ SAM and the $[Os(bpy)_2(bpy\text{-}C_{13}SH)]^{2-}$ and $CH_3(CH_2)_{11}SH$ (1 : 0.5) binary SAM in various supporting electrolytes at 0.1 V s^{-1}

Electrolytes[a]	$[Os(bpy)_2(bpy\text{-}C_{13}SH)]^{2-}$ SAM			Binary SAM[b]		
	E_p^{ox}/V	ΔE_p/mV	ΔE_{fwhm}/mV	E_p^{ox}/V	ΔE_p/mV	ΔE_{fwhm}/mV
KPF_6	0.69	68	207	0.66	8	143
$HClO_4$	0.69	30	142	0.68	3	129
$NaClO_4$	0.69	38	166	0.68	1	136
KNO_3	0.75	34	B	0.72	11	157
H_2SO_4	0.79	56	B	0.77	6	131

[a] Electrolytes solution were 0.1 M except for H_2SO_4, which was 0.05 M. [b] Binary SAM with $[Os(bpy)_2(bpy\text{-}C_{13}SH)]^{2-}$ and $CH_3(CH_2)_{11}SH$.

tial from 0.2 to 0.9 V. Figure 3 shows the variation of surface coverage versus cycling time measured in 0.1 M $NaClO_4$ at 0.1 V s^{-1}. It shows that the coverage decreases slowly to reach 75% of the full coverage after 40 minutes and does not decrease considerably since then. In the case of $[Os(bpy)_2(bpy\text{-}C_5SH)]^{2+}$ SAM (not shown here), the coverage decreased much more rapidly. Thus, the SAM electrodes are not considered sufficiently stable or durable to utilize in the long-term experiments.

It is needed to enhance the stability of the SAM electrodes. Considering the stability of the $[Os(bpy)_2(bpy\text{-}CnSH)]^{2+}$ SAMs, they have a different point such that the end group is much larger than that of the simple alkylthiol SAMs. This can result in significant structural difference in $[Os(bpy)_2(bpy\text{-}CnSH)]^{2+}$ SAMs. The distance between the nearest gold atoms in Au(111) surface is about 3 Å and adsorption of the alkylthiols usually takes place on the hollow sites which are about 5 Å apart from the nearest hollow site since the cross section of the alkylthiol chain is smaller than 5 Å. At this distance, the interactions between the nearest alkyl chains are compromised to form the compact and stable packing. It is common to monitor the STM images of alkylthiols showing $(\sqrt{3}\times\sqrt{3})R30^\circ$ packing pattern in which the distance between the nearest alkylthiols is *ca.* 5 Å. In this case, the alkyl chains are believed to have the conformation of all-*trans*. The situation in $[Os(bpy)_2(bpy\text{-}CnSH)]^{2+}$ SAMs, however, is quite different. Although in $[Os(bpy)_2(bpy\text{-}CnSH)]^{2+}$ molecules have alkyl backbones and thiol groups, the diameter of $[Os(bpy)_3]^{2-}$ moiety, about 12 Å, is much larger than the distance between the hollow sites. Therefore, ideal adsorption of in $[Os(bpy)_2(bpy\text{-}CnSH)]^{2-}$ molecules can take place on every third hollow sites because of the large diameter of in $[Os(bpy)_2(bpy\text{-}CnSH)]^{2+}$. If it is the case, the repulsion between the nearest alkyl chains is diminished a lot because the van der Waals interaction between the alkyl chains is expressed as a function of r^{-6}, where r is the distance. It might not be possible for $[Os(bpy)_2(bpy\text{-}CnSH)]^{2+}$ molecules to stand straight forming a compact packing at this distance. The decreased lateral repulsion allows elongated alkyl chains to contract to make kinks or gauche conformations. It is because there are empty spaces around the molecule. The loose packing is also the reason of the unstable SAMs because the $[Os(bpy)_2(bpy\text{-}CnSH)]^{2-}$ molecules experience little attraction from the surrounding $[Os(bpy)_2(bpy\text{-}CnSH)]^{2+}$ molecules and the possibility of desorption increases as a result.

If $[Os(bpy)_2(bpy\text{-}CnSH)]^{2+}$ molecules packed with the gauche conformations, the redox centers will not be located in a constant height, which results in diverse electron transfer possibility. Moreover, $[Os(bpy)_2(bpy\text{-}CnSH)]^{2-}$ molecules can adsorb at the nearer sites because the adsorption between the sulfur atom and adsorption site is much stronger than the lateral interaction and the resultant SAM can not be uniform.

The reorganization of the SAM is usually observed during the first cycle. It might be an evidence of the irregular packing since the cyclic voltammograms are surface morphology specific.

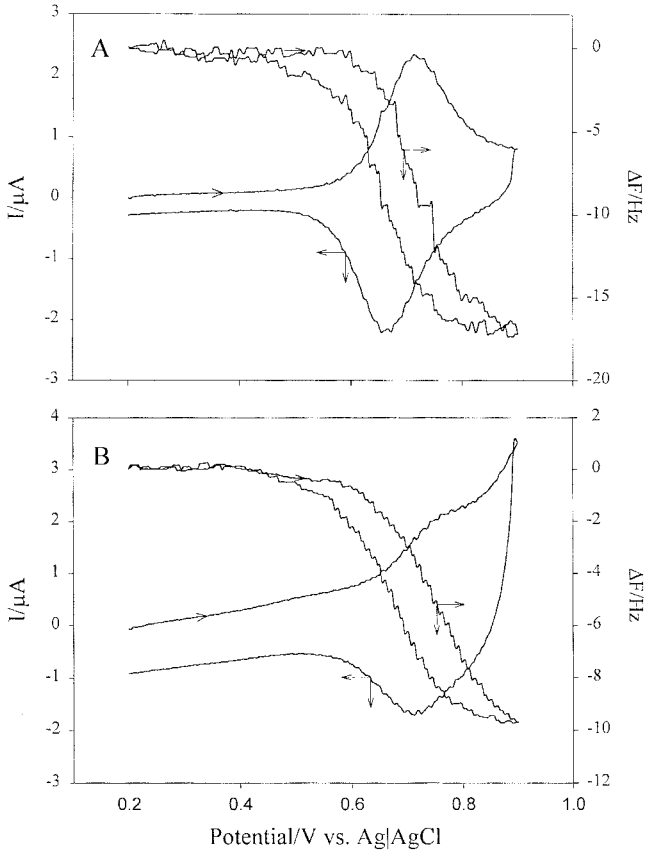

Figure 4. Electrochemical microgravimetric response obtained at a $[Os(bpy)_2(bpy\text{-}C_{13}SH)]^{2+}$ SAM electrode. Scan Rate: 0.1 V s^{-1}. Supporting electrolytes: (A) 0.1 M $HClO_4$, and (B) 0.05 M H_2SO_4.

Microgravimetric Determination of Hydration Numbers of Counteranions. The electrochemical microgravimetry measurements were carried out for studying the transport of counter anions. Upon oxidation of the immobilized complexes, the influx of counter anion into the monolayer is required to neutralize the additional charge generated. As shown in Figure 4, an increase in mass is observed as expected during the positive scan. The mass began to increase along with the flow of oxidation current and continued to increase up to the positive limit. After the scan direction was switched back at 0.9 V, the mass decreased and then returned to the initial value when the reduction current ceased to flow. Recovery of the mass to its initial value means that the electron transfer and anion-association are reversible. The time delay from the onset of current to the mass change is quite short unlike the cases of thin polymer films.[36] It is explained as the SAM is very thin and the counter ions can be associated or dissociated through electrostatic interactions immediately responding to the applied electrode potential. The mass changes are independent of the scan rates from 20 to 100 mV s^{-1}.

This change is dominated by anions that are expected to move in the hydrated form. It is because the estimated mass from the oxidation or reduction charge is smaller than the mass obtained by the electrochemical microgravimetry. Comparing the cyclic voltammogram to the calculated current curve resulting from differentiation of the frequency curve

gives the information on the hydration number of the counter ions. It gives the hydration numbers of the electrolyte anions as 16±2, 11±1, 5±1 and 24±6 for ClO_4^-, PF_6^-, NO_3^-, and SO_4^{2-} respectively.

However, the maximum frequency change is less than 20 Hz and the frequency data contain fluctuation acting as noises in the process of data treatment. The resultant current curve or the differentiated frequency curve has a noisy background, which prohibits the correct result. To overcome this problem, we attempted to fit the cyclic voltammogram with the equation for the thin-layer cell.[45] Though it is a very rough approximation, but considered to be useful for estimation of the hydration numbers. For this calculation, we took the peak current value from the CV. The formal potential was taken from the frequency data because it is exact and easy to extract compared with the value from the CV with a skewed baseline and large background especially in the anodic region. We used ΔE_{fwhm} value as a variable. Actually $\Delta E_{fwhm} = 3.53RT/nF = 90.6/n$ mV for an ideal nernstian reaction at 298 K under the Langmuir adsorption conditions with no lateral interaction in the SAM. R is the gas constant, T is the absolute temperature. F is the Faraday constant, and n is the number of mole of transferred electrons. Since the actual ΔE_{fwhm} value measured in the cyclic voltammogram is larger than the ideal value, we put $\Delta E_{fwhm}/3.53$ instead of RT/F. Integration of the resultant curve (Figure 5) and comparison with the frequency data give the hydration number. The calculated hydration numbers are 16, 10, 12 and 21 for ClO_4^-, PF_6^-, NO_3^-, and SO_4^{2-}, respectively. The calculated values are in good agreement with the values obtained from comparing CV with differentiated frequency data.

Binary SAMs of $[Os(bpy)_2(bpy\text{-}C_{13}SH)]^{2+}$ and dodecanethiol. For the enhancement of the stability and the regularity of SAMs, insertion of alkylthiols around the adsorbed $[Os(bpy)_2(bpy\text{-}CnSH)]^{2-}$ molecules was attempted using a mixed solution of alkylthiol and $[Os(bpy)_2(bpy\text{-}CnSH)]^{2-}$ in preparation of SAMs. The binary SAMs composed of $[Os(bpy)_2(bpy\text{-}C_{13}SH)]^{2-}$ and the electroinactive species, $CH_3(CH_2)_{11}SH$, were prepared in a solution of $[Os(bpy)_2(bpy\text{-}C_{13}SH)]^{2-}$ and $CH_3(CH_2)_{11}SH$ (1 : 0.1 or 1 : 0.5). Hereafter the binary SAMs are called 1 : 0.1 SAM or 1 : 0.5 SAM after the composition of the solutions used to prepare the SAM. The electrochemical behavior of the binary SAMs was examined.

Figure 6 shows the CV for the binary SAM electrode, which represents the reduced background current compared with the result of an $[Os(bpy)_2(bpy\text{-}C_{13}SH)]^{2-}$ SAM exhibited in Figure 2. First of all, it is worthy to note that the anodic peak position shifted to the negative direction as much as the cathodic peak and the redox peak shape of a binary SAM becomes more symmetrical, which means that the molecular packing in the monolayer is made better. The ΔE_p° and ΔE_{fwhm} values of the binary SAMs are much smaller than those of $[Os(bpy)_2(bpy\text{-}C_{13}SH)]^{2+}$ SAM. This effect is outstanding especially in 0.05 M H_2SO_4.

In a binary SAM prepared in the 1 : 0.5 solution, the ΔE_p values decreased to few mV which is almost an order smaller value than those of $[Os(bpy)_2(bpy\text{-}C_{13}SH)]^{2-}$ SAM, meaning the electron transfer rate is very fast. The fact that ΔE_{fwhm} decreased significantly means the much-relieved repulsion in the monolayer. Besides, the repulsion in sulfuric acid and perchloric acid medium is almost the same. These changes are attributed to the enhanced packing or variations in struc-

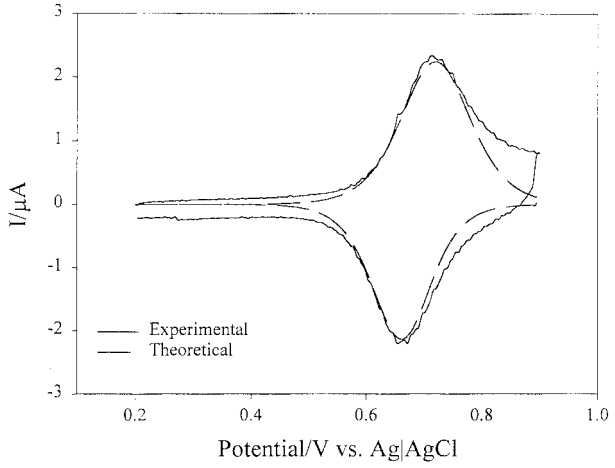

Figure 5. Simulated current curve matching the cyclic voltammogram well. The peak current was taken from the CV and the formal potential, E_p°, was taken from the frequency. For detailed explanation, see the text.

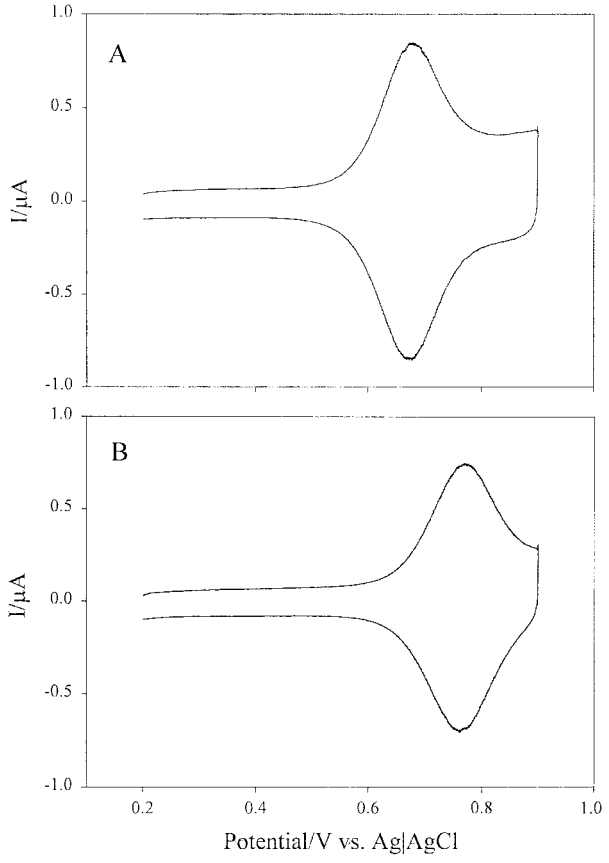

Figure 6. Cyclic voltammograms of a binary SAM composed of $[Os(bpy)_2(bpy\text{-}C_{13}SH)]^{2+}$ and $CH_3(CH_2)_{11}SH$ prepared in (a mole ratio of 1 : 0.5 in the adsorbing solution) in (A) 0.1 M $HClO_4$, and (B) 0.05 M H_2SO_4 recorded at 0.1 V s^{-1}.

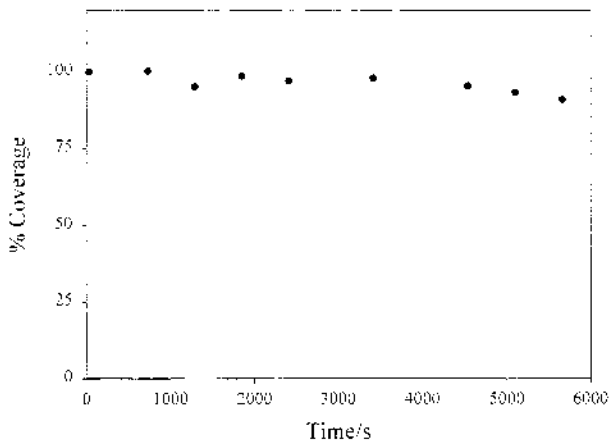

Figure 7. Variation of surface coverage of a mixed SAM electrode measured in 0.1 M $NaClO_4$ during repetitive potential cycling at 0.1 V s^{-1}. After 1.5 h the coverage was decreased to 91% of the initial value, which shows the mixed SAM quite stable.

ture that give rise to a range of closely spaced formal potential values rather than a single value.

The surface coverage decreased without a doubt because the concentration of $[Os(bpy)_2(bpy\text{-}C_{13}SH)]^{2-}$ is diluted. For the 1 : 0.5 binary SAM. the coverage is found in 0.1 M $HClO_4$ to be about 4.0×10^{-11} mol cm^{-2} while it is 1.3×10^{-10} mol cm^{-2} for the $[Os(bpy)_2(bpy\text{-}C_{13}SH)]^{2+}$ SAM. It means the surface coverage of 30% was achieved with the solution diluted by 67% with the spacer molecules. We found this ratio is practically the optimum value for this case.

For the SAM prepared in a more concentrated solution, that is. the $[Os(bpy)_2(bpy\text{-}C_{13}SH)]^{2+}/CH_3(CH_2)_{11}SH$ (1 : 0.1) solution. the values of $E_p°$, ΔE_p, and ΔE_{fwhm} for the redox waves changed also. but the change is rather small. In 0.1 M $HClO_4$. ΔE_p is just 18 mV while it decreased to 28 mV for 0.05 M H_2SO_4. These are still larger than those from the concentrated solutions.

The stability of the SAM was tested by cycling the potential from 0.2 to 0.9 V as we did in Figure 3. Figure 7 shows that the coverage decreases slowly to reach 97% of the full coverage after 40 minutes and does not decrease considerably ever after. The binary SAM is stable enough to utilize in the long time experiments compared with the $[Os(bpy)_2(bpy\text{-}C_{13}SH)]^{2-}$ SAM.

Regarding the microgravimetric measurements, the frequency curves are similar to that shown in Figure 4 except that the frequency changes are less than 10 Hz. The same treatment as described in the previous section gives rise to the hydration numbers of the electrolytes. The hydration numbers obtained using a binary SAM are almost same as presented above.

In summary, the typical coverage value for the $[Os(bpy)_2(bpy\text{-}C_{13}SH)]^{2-}$ SAM is 1.3×10^{-10} mol cm^{-2} and the adsorption seemed to be strongest in 0.05 M H_2SO_4 compared to that in other electrolytes. The electron transfer in this SAM is retarded somewhat when the scan rate is lower than 2 V s^{-1}. In 0.1 M $HClO_4$, the ΔE_{fwhm} values are larger than the theoretical value, which exhibits that there are repulsive interactions in the SAM. By EQCM measurements at the $[Os(bpy)_2(bpy\text{-}C_{13}SH)]^{2-}$ SAM. the hydration numbers of the electrolyte anions could be determined as 16 ± 2, 11 ± 1, 5 ± 1 and 24 ± 6 for ClO_4^-. PF_6^-. NO_3^-, and SO_4^{2-}, respectively. For the binary SAMs that were prepared by co-adsorption of alkylthiols, the stability and the electrochemical reversibility was enhanced. Especially in a 1 : 0.5 binary SAM, the repulsion in SAM is much reduced and the electron transfer rate is very fast. The coverage determined in 0.1 M $HClO_4$ is about 4.0×10^{-11} mol cm^{-2}. The coverage doe not change much even after a repetitive potential cycling for 90 min while the $[Os(bpy)_2(bpy\text{-}C_{13}SH)]^{2+}$ SAM shows 25% desorption under similar condition.

Acknowledgment. This work was supported by the Korea Science and Engineering Foundation (KOSEF) (981-0307-036-2 and 1999-2-121-003-4) and in part by the Basic Research Science Program. Ministry of Education. Project No. BSRI-98-3430. GB acknowledges KRF for the financial support through the Young Student Support Program. We are grateful to Prof. Chang and Sim. Dr. Moon for syntheses of 4-methyl-4'-alkanethiol-bipyridyls.

References

1. *Molecular Design of Electrode Surface: Techniques of Chemistry Series*; Murray, R. W., Ed.; Wiley: New York, 1992; Vol. 22.
2. Ulman, A. *An Introduction to Ultra Thin Organic Films from Langmuir-Blodgett to Self-Assembly*; Academic Press: New York, 1991.
3. (a) Chidsey, C. E. D.; Bertozzi, C. R.; Putvinski, T. M.; Mujsce, A. M. *J. Am. Chem. Soc.* **1990**, *112*, 4301. (b) Chidsey, C. E. D.; Loiacono, D. *Langmuir* **1990**, *6*, 682. (c) Chidsey, C. E. D. *Science* **1991**, *251*, 919. (d) Collard, D. M.; Fox, M. A. *Langmuir* **1991**, *7*, 1192. (e) Hickman, J. J.; Ofer, D.; Laibinis, P. E.; Whitesides, G. M.; Wrighton, S. *Science* **1991**, *252*, 688.
4. (a) Nuzzo, R. G.; Allara, D. L. *J. Am. Chem. Soc.* **1983**, *105*, 4481. (b) Porter, M. D.; Bright, T. B.; Allara, D. L.; Chidsey, C. E. D. *J. Am. Chem. Soc.* **1987**, *109*, 3559. (c) Bain, C. D.; Troughton, E. B.; Tao, Y-. T.; Evall, J.; Whitesides, G. M.; Nuzzo, R. G. *J. Am. Chem. Soc.* **1989**, *111*, 321. (d) De Long, H. C.; Buttry, D. A. *Langmuir* **1990**, *6*, 1319.
5. (a) Finklea, H. O.; Avery, S.; Lynch, M.; Furtsch, T. *Langmuir* **1987**, *3*, 409. (b) Hautman, J.; Kelvin, M. *J. Chem. Phys.* **1989**, *91*, 4994.
6. (a) Finklea, H. O.; Hanshew, D. D. *J. Am. Chem. Soc.* **1992**, *114*, 3173. (b) Bain, C. D.; Whitesides, G. M. *Langmuir* **1989**, *5*, 1370. (c) Ulman, A.; Evans, S. D.; Shnidman, Y.; Sharma, R.; Eilers, J. E.; Chang, J. C. *J. Am. Chem. Soc.* **1991**, *113*, 1499.
7. Abbott, N. L.; Folkers, J. P.; Whitesides, G. M. *Science* **1992**, *257*, 1380.
8. Chidsey, C. E. D.; Loiacono, D. N. *Langmuir* **1990**, *6*, 682.
9. Rowe, G. K.; Creager, S. E. *Langmuir* **1991**, *7*, 2307.
10. Bard, A. J.; Abruna, H. D.; Chidsey, C. E. D.; Faulkner, L. R.; Feldberg, S.; Itaya, K.; Majda, M. M.; Melroy, O.; Murry, R. W.; Porter, M.; Soriaga, M.; White, H. S. *J.*

Phys. Chem. **1993**, *97*, 7147.
11. Thomas, R. C.; Houston, J. E.; Michalske, T. A.; Crooks, R. M. *Science* **1993**, *259*, 1883.
12. Atre, S. V.; Liedberg, B.; Allara, D. L. *Langmuir* **1995**, *11*, 3882.
13. Yan, L.; Marzolin, C.; Terfort, A.; Whitesides, G. M. *Langmuir* **1997**, *13*, 6704.
14. Rojas, M. T.; Kaifer, A. E. *J. Am. Chem. Soc.* **1995**, *117*, 5883.
15. Rowe, G. K.; Creager, S. E. *J. Phys. Chem.* **1994**, *98*, 5500.
16. Acevedo, D.; Abruna, H. D. *J. Phys. Chem.* **1991**, *95*, 9590.
17. Acevedo, D.; Bretz, R. L.; Tirado, J. D.; Abruna, H. D. *Langmuir* **1994**, *10*, 1300.
18. Tender, L.; Carter, M. T.; Murray, R. W. *Anal. Chem.* **1994**, *66*, 3173.
19. Carter, M. T.; Rowe, G. K.; Richardson, J. N.; Tender, L. M.; Terrill, R. H.; Murray, R. W. *J. Am. Chem. Soc.* **1995**, *117*, 2896.
20. Forster, R. J.; OKelly, J. P. *J. Phys. Chem.* **1996**, *100*, 3695.
21. Smalley, J. F.; Feldberg, S. W.; Chidsey, C. E. D.; Linford, M. R.; Newton, M. D.; Liu, Y. *J. Phys. Chem.* **1995**, *99*, 13141.
22. Kim, N.; Kim, Y.-G.; Kim, S. H.; Jeon, I. C. manuscript in preparation.
23. Guiomar, A. J.; Guthrie, J. T.; Evans, S. D. *Langmuir* **1999**, *15*, 1198.
24. Atre, S. V.; Liedberg, B.; Allara, D. L. *Langmuir* **1995**, *11*, 3882.
25. Kim, Y.-G.; Kim, N.; Kim, S. H.; Jeon, I. C. *Proc. STM'97*; Hamburg, Jul. 25-30, 1997; p 237.
26. Kim, S. H.; Lee, S. H.; Kang, S. H. *Tetrahedron Lett.* **1998**, *39*, 9693.
27. De Long, H. C.; Donohue, J. J.; Buttry, D. A. *Langmuir* **1991**, *7*, 2196.
28. Creager, S. E.; Rowe, G. K. *Anal. Chim. Acta* **1991**, *246*, 233.
29. Bretz, R. L.; Abruna, H. D. *J. Electroanal. Chem.* **1995**, *388*, 123.
30. Shimazu, K.; Yagi, I.; Sato, Y.; Uosaki, K. *J. Electroanal. Chem.* **1994**, *372*, 117.
31. Sato, Y.; Mizutani, F.; Shimazu, K.; Ye, S.; Uosaki, K. *J. Electroanal. Chem.* **1997**, *434*, 115.
32. Takada, K.; Abruna, H. D. *J. Phys. Chem.* **1996**, *100*, 17909.
33. Moon, J.-M. *Ph.D. Thesis*: Jeonbuk National University, Jeonju, KOREA, 2000.
34. MS for $[Os(bpy)_2(bpy\text{-}C_5SH)](PF_6)_2$ adsorbed on Au: $[M\text{-}2(PF_6)]$ + Au = 974, UV-VIS for $[Os(bpy)_2(bpy\text{-}C_{13}SH)](PF_6)_2$ in methanol: 245, 291, 331, 370, 437, 482 nm.
35. NMR for $[Os(bpy)_2(bpy\text{-}C_{13}SH)](PF_6)_2$ in Acetone-d6 (chemical shift, ppm): 1.27 (m, 20H), 1.71 (t, 2H), 2.56 (t, 2H), 2.86 (t, 1H), 3.04 (s, 3H), 7.32 (q, 1H), 7.45 (d, 2H), 7.74 (d, 1H), 7.94 (m, 4H), 8.72 (s, 1H), 8.80 (d, 2H).
36. Shin, M.; Kim, E.; Kwak, J.; Jeon, I. C. *J. Electroanal. Chem.* **1995**, *394*, 87.
37. Karpovich, D. S.; Blanchard, G. J. *Langmuir* **1994**, *10*, 3315.
38. Huang, X.; Kovaleski, J. M.; Wirth, M. J. *Anal. Chem.* **1996**, *68*, 4119.
39. Abruna, D. D. In *Electroresponsive Molecular and Polymeric Systems;* Skotheim, T. A., Ed.; Marcel Dekker: New York, 1988.
40. Brown, A. P.; Anson, F. C. *Anal. Chem.* **1977**, *49*, 1589.
41. Matsuda, H.; Aoki, K.; Tokuda, K. *J. Electroanal. Chem.* **1987**, *217*(1), 15.
42. Thomas, R. C.; Sun, L.; Crooks, R. M. *Langmuir* **1991**, *7*, 620.
43. Chen, S. H.; Frank, C. F. *Langmuir* **1989**, *5*, 9778.
44. Sauvage, J.; Collin, J.; Chambron, J.; Guillerez, S.; Coudret, C.; Balzani, V.; Barigelletti, F.; Cola, L. D.; Flamigni, L. *Chem. Rev.* **1994**, *94*, 993.
45. Bard, A. J.; Faulkner, L. R. *Electrochemical Methods Fundamentals and Applications;* Wiley: New York, 1980.